Available online at www.eccomasproceedia.org
Eccomas Proceedia COMPDYN (2021) 2359-2365

ECCOMAS
Proceedia

COMPDYN 2021
8th ECCOMAS Thematic Conference on
Computational Methods in Structural Dynamics and Earthquake Engineering
M. Papadrakakis, M. Fragiadakis (eds.)
Streamed from Athens, Greece, 28 - 30 June 2021

TIMBER BEAM-TO-COLUMN JOINT WITH STEEL LINK: DESIGN AND MECHANICAL CHARACTERIZATION THROUGH NUMERICAL INVESTIGATION

G. Iovane, B. Faggiano*

University of Naples Federico II, Dept. Structures for Engineering and Architecture
Via Claudio 21, 80125, Naples, Italy
giacomo.iovane@unina.it, faggiano@unina.it

Abstract

For the design of dissipative heavy timber frame structures, in the context of modern seismic design approach based on the mechanical triad of strength, stiffness and ductility, brittle timber failure modes can be avoided by integrating hybrid timber-steel system into modern timber connection technology. Thus, the overall seismic performance of timber structures can be improved, entrusting the dissipation function to ad hoc conceived devices, like steel links.
With reference to the structural type of Moment Resisting Frames (MRF), steel links located at the ends of the beams are able to provide a significant dissipative capacity, by means of cycles of plastic deformations, while timber members and steel connections, to be designed with an adequate overstrength as respect to the link, behave in elastic field.
In this regards, the paper presents the capacity design and the mechanical characterization through monotonic numerical analyses of two different timber beam-to-column joint with steel link for MRF structures, consisting of a timber beam and a steel link connected each other by means of a stiffened end-plate and glued-in steel rods.
The proposed design criteria of the joint are validated through the evaluation of performance, by means of nonlinear pushover analyses on the joint refined FEM models, in terms of key parameters, such as ultimate resistance, stiffness, rotation capacity and failure modes. The numerical results confirm the plastic deformation of the link, which large dissipative capacity of the joint corresponds to.

Keywords: Seismic resistant timber structures, beam-to-column joints for dissipative timber moment resisting frames, steel link, component method for timber joints, capacity design for timber structures, FEM analysis of beam-to column joints for timber MRFs.

ISSN:2623-3347 © 2021 The Authors. Published by Eccomas Proceedia.
Peer-review under responsibility of the organizing committee of COMPDYN 2021.
doi:10.7712/120121.8642.19355

1 INTRODUCTION

Toward the dissipative seismic resistant timber structures design, steps must be taken to overcome the seismic deficiencies related to the inherent fragility of wood. Since timber is a material with an elastic-fragile behavior, in the present anti-seismic regulations, such as in Europe the Eurocode 8 [1], it is indicated that the joints could dissipate through the plastic deformations of metallic connectors. However, joints are structural elements with an important role in bearing the design loads. In view of the development of heavy timber seismic resistant structures, in the context of modern seismic design approach based on the mechanical triad of strength, stiffness and ductility, the dissipative capabilities should be delegated to specific devices [2]. In fact, by integrating modern steel connection technology into timber system, brittle wood failure modes can be avoided and the overall seismic performance of timber structures can be improved. Some recent research has focused on the development of hybrid timber-steel, instead of relying on an all-timber structure, showing good potential for improving the behaviour of seismic resistant timber structures [2-4]. Very efficient solutions are steel links, to be located in timber members depending on the seismic resistant structural type, which are able to provide a significant dissipative capacity, by means of cycles of deformations in plastic field, if designed with adequate strength, stiffness and ductility.

It is therefore possible to take advantage of the knowhow on steel constructions related to the seismic design criteria, according to the approach based on the ductile and dissipation requirements (capacity design), adopting necessary adaptations corresponding to the peculiarities of timber, which should be based on the calibration of the fundamental parameters. With reference to the structural types of Moment Resisting Frames (MRF), steel links located at the ends of the beams [5-12] have the function of ductile fuses, where the plastic hinge in bending is concentrated, while the timber members should be designed with an adequate overstrength, to remain in elastic field. Recently Montuori and Sagarese [9] have applied the steel reduced beam sections, commonly proposed for steel MR frames [10, 11], to timber beams.

The crucial aspect is the design of joints. In timber structures engineering this issue is certainly innovative, it requiring a significant detailed study aimed at characterizing the mechanical behavior of connections in terms of stiffness, strength and ductility.

In this regards the paper focuses on the design of two beam to column timber joints, with the same configuration, equipped with different steel links, for dissipative heavy timber MRF. It illustrates a part of a wider study, including both numerical and experimental investigations on either joints or whole structural systems.

The joints are designed through the capacity design approach, by applying the component method, with the aim to allow the plastic hinge formation in the steel links, while the timber member and the connections are designed to remain elastic, with adequate overstrength.

The mechanical characterization of the joints is carried out through monotonic numerical analyses, on refined FE models, already calibrated upon past experimental tests [8], by means of the structural calculation program ABAQUS FEA (2019). As a result, the numerical F-u (vertical force-displacement) and M-θ (bending moment-rotation) curves obtained are compared to evaluate the capabilities of the joints and the adequacy of the proposed design criteria.

2 DISSIPATIVE JOINTS DESIGN

2.1 Design criteria of the joint

The detail of the configuration of the beam-to-column joint with steel link under study is shown in Figure 1a. In particular the steel link is connected to the timber members by means of bolted endplates stiffened by triangular plates. The capacity design is applied on two levels

[12]: for macro-components, they being timber beam and column, steel link, connection between link and timber members, so that timber members and connections have an over strength as respect to the steel link; for sub-components, they being timber members, steel link, connection elements, such as, end-plate, stiffeners and steel bars, imposing a collapse hierarchy of components for achieving an overall ductile failure of the joint (Fig. 1).

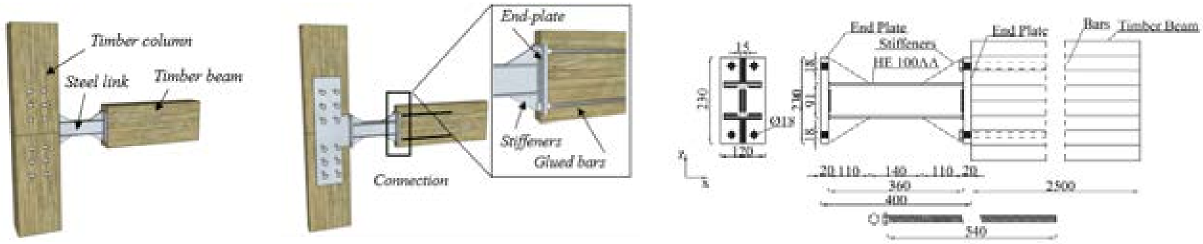

Figure 1: a) Identification of the joint components; b) the reference joint [mm; 12].

With regards to the capacity design for macro-components, the dissipative link should be designed in order to achieve a pure bending behavior, so that the full plastic bending resistance and the rotation capacity of the dissipative link should be not affected by axial and shear forces (Eurocode 3 (EC3) part 1-1[13]. At the same time, the link cross sections should have high ductility, according to EC8 [1]. For non-dissipative elements, such as timber beams and columns, the capacity design criterion should be satisfied, according to EC8 [1].

With regards to the capacity design for sub-components, according to the component method (EC3 part 1-8 [13]) the joint is assumed as an assembly of components, whose mechanical behavior is studied separately, taking into consideration the contribution of each one in terms of strength, stiffness and rotation. The link to column connection is assumed as rigid.

The design bending resistance of the joint is determined as it follows [12]:

$$M_{i,Rd} = F_{i,Rd} \cdot z \tag{1}$$

where z is the lever arm of the resistant bending moment (Fig. 2) and $F_{i,Rd}$ is the resistance of the weakest joint component, such as the smallest value among the following ones, where the stiffened endplate is studied as an equivalent T-stub (Fig. 2b, c; EC3 part 1-8 [13]).

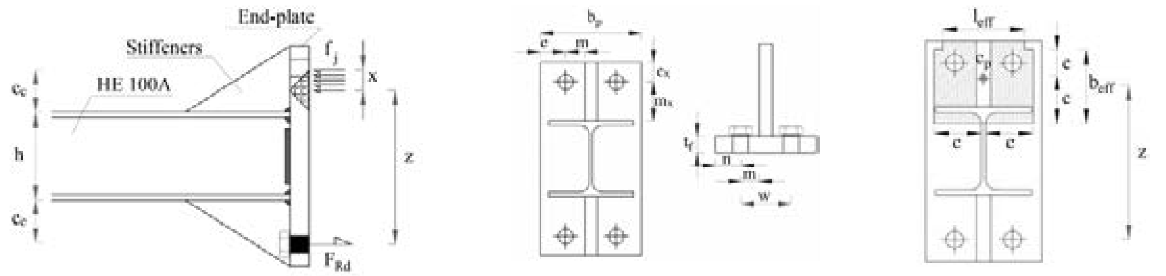

a) Stiffened endplate joint b) T-Stub in tension c) T-Stub in compression

Figure 2: Joint models [13].

For the T-stub in tension (Fig. 2b), $F_{t,T\text{-}stub,Rd}$ is the minimum contribution provided by the following possible failure modes (EC3 part 1-8 [13]: 1) complete yielding of the flange; 2) bars failure with yielding of the flange in presence of prying forces; 3) bar failure in tension.

For the T-stub in compression (Fig. 2c; EC3 part 1-8 [13], $F_{c,T\text{-}stub,Rd}$ is evaluated with reference to an effective compression area, assuming the compression centre (c_p) approximately located at the centroid of the T section identified by the stiffener and the steel link flange.

For the steel stiffeners, $F_{s,Rd}$ is determined through the equivalent truss model [14], which defines the equivalent strut area of the stiffener, with a possible yielding failure mode.

For the glued-in steel bars in tension (pull-out; CNR-DT 206 R1/2018 [15]), $F_{ax,Rd}$ is evaluated with reference to the following possible failure modes: a) bar failure in tension; b) failure for debonding at the adhesive to timber interface; c) failure of timber in tension; d) failure of timber for splitting in the bar direction. The latter can be avoided by respecting the minimum distances from the edge and minimum spaces between the glued bars in tension [15].

2.2 The joints studied

The reference joint [12] is shown in Figure 1b. New link devices are here adopted, such as HE100A (Fig. 3a) and IPE100 (Fig. 3b) steel profiles. The hierarchy resistance criteria are applied to design the joints components (timber beam, end-plate, stiffeners, bars). Definitely the two study joints have the features shown in Figure 3, they also differ for the endplates thickness, they being 20 and 15 mm thick, respectively. Material grades are given in Figure 4.

In Table 3 the results of the joints design are presented. The outputs are provided for the joint components in terms of design resistance $F_{i,Rd}$, bending resistance $M_{i,Rd}$ (eq. 1) and overstrength (OS_i), evaluated as the ratio $M_{i,Rd}/M_{l,pl,Rd}$, where $M_{l,pl,Rd}$ is the bending design resistance of the link. It is apparent that the dissipative link is the first component to reach the elastic limit (yielding). Moreover the overstrength coefficient of the timber beam as respect to the link is larger for the IPE100 device and the collapse hierarchy changes for the two cases.

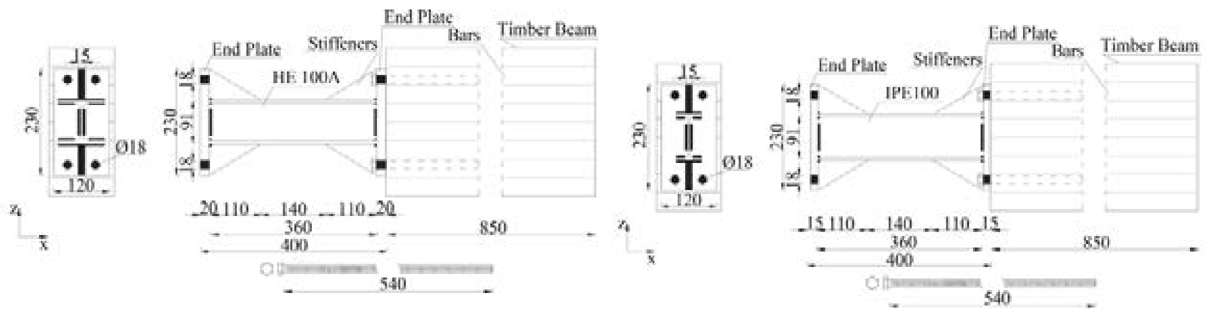

Figure 3: Geometrical features: a) HE100A and b) IPE100 joints.

HE100A				IPE100			
Collapse hierarchy	$F_{i,Rd}$ [kN]	$M_{i,Rd}$ [kNm]	OS_i [%]	Collapse hierarchy	$F_{i,Rd}$ [kN]	$M_{i,Rd}$ [kNm]	OS_i [%]
Link yielding	/	26	1,00	Link yielding	/	12	1
Pull-out (Mode d)	137	27	1,04	Stiffners yielding	89	17	1,43
Stiffners yielding	183	35	1,35	T-stub in tension (Mode 1)	132	26	2,12
Pull-out (Mode c)	208	40	1,53	Pull-out (Mode d)	137	27	2,19
T-stub in tension (Mode 1)	219	42	1,61	T-stub in compression	165	32	2,64
T-stub in compression	220	42	1,62	Pull-out (Mode c)	208	40	3,39
Bar failure in tension	226	43	1,66	Bar failure in tension	226	43	3,62
Timber beam in bending	/	50	1,95	Timber beam in bending	/	50	4,16

Table 3: Study joints: collapse hierarchy, design force ($F_{i,Rd}$) and bending resistance ($M_{i,Rd}$), over-strength (OS_i).

3 MECHANICAL CHARACTERIZATION OF THE JOINTS

3.1 Monotonic numerical analysis

The mechanical behavior of the HE100A and IPE100 joints is examined through a monotonic nonlinear numerical analysis through the software ABAQUS FEA (2019). The implicit dynamic analysis is performed applying a load history in displacement control. The displacement is imposed at the end of the cantilever beam, with increment of 20mm up to collapse, corresponding to the test speed of 0,2 mm/s [16]. The F-u and M-θ curves are drawn to evaluate the global and local behavior of the joints. In particular, the bending moment at the joint (M) and the corresponding rotation (θ) are evaluated at the mid section of the link; the displacement (u) in z-direction is evaluated at the applied force (F) section (Fig. 4a).

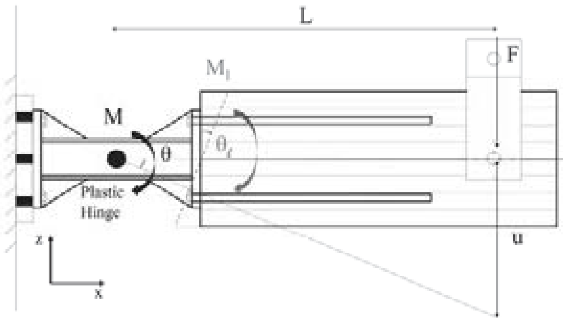

Component	Beam	Bars	End-Plates	Link
Material	Timber		Steel	
	GL24h	10.9	S275	S355
ρ [N/mm^3]	3,80 e^{-6}		7,85 e^{-5}	
E [MPa]	E_0=390 E_{90}=11600		210000	
σ_{el} [MPa]	24	900	275	255
σ_u [MPa]	/	1000	430	510
ε_u [MPa]	/	0,178	0,376	0,261

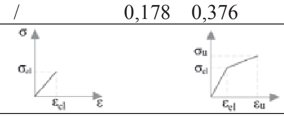

Figure 4: a) Geometric model and performance parameters of the joint; b) Materials features: density (ρ), elastic modulus (E), elastic (σ_{el}) and ultimate resistance (σ_u) resistance, elastic (ε_{el}) and ultimate (ε_u) strains.

With regard to the material models, timber is assumed with an elastic fragile behavior, while for end-plate, bolts and link steels an isotropic hardening model is adopted, according to EC3 part 1-1 ([13] Fig. 4b), and true stress-true strain equations.

In Figure 5 the Force-displacement (F-u) and Moment-rotation (M-θ) curves of the HE100A and IPE100 joints are presented and compared. Specific performance points are evidenced, corresponding to the link yielding (P_Y), full plasticization (P_P) and ultimate strength (P_C), as collapse condition and the end of the numerical analysis, it corresponding to the buckling of the link web (HE100A) or flange (IPE100).

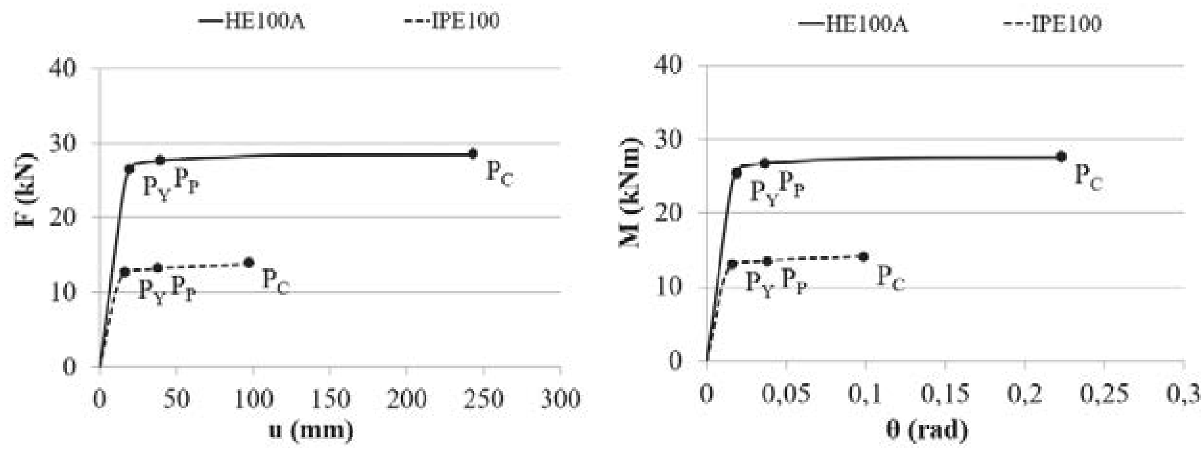

Figure 5: F-u and M-θ curves; performance points: Y-yielding, P- plasticization, C- collapse.

It is observed that the HE100A joint has greater stiffness, strength and ductility as respect to the IPE100 joint thanks to the link steel profile and the larger end-plate thickness. In both joints the plastic deformation of the link occurs, achieving the formation of the plastic hinge.

3.2 Analysis of results

The stress distribution in the joint and the AC yield (Actively Yielding) distribution that identifies the attainment of yield stresses in the joint are shown in Table 5 at the collapse condition, where the maximum stress value (σ_{max}) of each joint component is also given.

	HE100A					IPE100				
	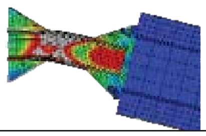			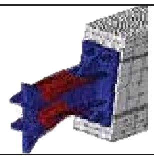		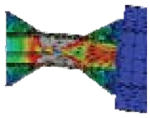			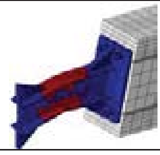	
	Link	End Plate	Threaded Bars	Timber beam	Stiffeners	Link	End Plate	Threaded Bars	Timber beam	Stiffeners
σ_{max}	438	260	537	11,9	299	402	222	308	7,5	289

Table 5: Stress [MPa] distributions and maximum value in the joint components at collapse P_C.

For each i-th component (end-plate, stiffeners, threaded bars or timber beam) of the joints, the demand capacity ratio ($DCR_{i,j,el}=\sigma_{i,j}/\sigma_{i,el}$) between the maximum stress value evaluated at P_C point ($\sigma_{i,PC}$) and the stress value at the elastic limit P_Y point ($\sigma_{i,el}$;) is provided in Table 6.

[%]	Link		End Plate		Thread Bars		Timber beam		Stiffeners	
	HE100A	IPE100	HE100A	IPE100	HE100A	IPE100	HE100A	IPE100	HE100A	IPE100
$DCR_{i,el,}$	123	113	95	81	60	34	50	31	109	105

Table 6: DCR [%] at P_C for HE100A and IPE 100 joints.

The following collapse hierarchy of the joint components is evidenced: Link web (HE100A) or flange (IPE100) buckle, thus inducing the joint collapse, stiffeners undergoes plastic deformation, while end-plate, bars and timber beam are still in elastic field.

4 CONCLUSIVE REMARKS

The paper focuses on beam to column joints with dissipative steel link in the beam for seismic moment resistant heavy timber framed structures. In particular, the capacity design is applied through the component method, defining a collapse hierarchy on two levels, macro-components and sub-components. For both the joints, the numerical non linear pushover analysis has confirmed both the formation of the plastic hinge in the link which dissipates the energy through plastic deformation and the collapse hierarchy of the joint components, validating both the efficiency of the system and the proposed design method.

Future developments include the numerical evaluation of the cyclic behavior of the joints. Moreover, experimental tests will allow to check the accuracy of the proposed design criteria and the calibration of the design parameters.

The topic is noteworthy, as background for the development of the chapter on seismic-resistant timber structures of the technical standards for constructions.

ACKNOWLEDGEMENT

The study is object of the Reluis/DPC 2019-2021 (WP3, Task 1) project.

REFERENCES

[1] EN 1998-1: 2004: Eurocode 8: Design of structures for earthquake resistance – Part 1: General rules, seismic actions and rules for buildings (CEN: Comité Européen de Nor-

malisation).

[2] Faggiano B., Iovane G.. First considerations on the design approach and criteria for seismic resistant moment resisting and bracings timber frames. J. Eberhardsteiner, W. Winter, A. Fadai, M. Pöll eds. *World Conference on Timber Engineering, (WCTE2016)*, Full paper ID1094, Vienna, Austria, August 22-25, 2016.

[3] Humbert J., Lee S.J., Park J.-S., Park M.-J.. Moment resistance of post-and-beam joints with concealed metallic connectors. A. Salenikovich ed., *World Conference on Timber Engineering (WCTE 2014)*, Quebec City, Canada, August 10-14, 2014.

[4] Komatsu K., Kitamori A., Mori T.. Evaluation on dynamic performance of glulam frame structure composed of slotted bolted connection system. A. Salenikovich ed., *World Conf. on Timber Engin.(WCTE 2014)*, Quebec City, Canada, August 10-14, 2014.

[5] Tomasi R., Zandonini R., Piazza M., Andreolli M.. Ductile end connections for glulam beams. *Structural Engineering International*, 18, 290-296, 2008.

[6] Andreolli M., Piazza M., Tomasi R., Zandonin R.. Ductile moment-resistant steel-timber connections. *Structures and Buildings*, 164 (SB2), 65-78, 2011.

[7] Gohlich R., Erochko J., Woods J.E.. Experimental testing and numerical modelling of a heavy timber moment-resisting frame with ductile steel links. *Earthquake Engineering & Structural Dynamics*, 47,1460-1477, 2018.

[8] Faggiano B., Iovane G., Tartaglia R., Ciccone G., Landolfo R., Mazzolani F.M., Andreoli M., Tomasi R., Piazza M.. Numerical simulation of monotonic tests on beam-column timber joints equipped with steel links for heavy timber seismic resistant MRF. *16th International Conference of Numerical Analysis and Applied Mathematics (ICNAAM 2018)*, doi.org/10.1063/1.5114268.

[9] Montuori R. and Sagarese V.. The use of steel RBS to increase ductility of wooden beams. *Engineering Structures*, 169, 154-161. 2018.

[10] Faggiano B., De Cesbron De La Grennelais E., Landolfo R.. Design criteria for RBS in MR frame retrofitting. *4th International Conference Behaviour of steel structures in seismic areas (STESSA 2003)*, 683-690, 2003.

[11] Montuori R.. The influence of gravity loads on the seismic design of RBS connections. *The Open Construction and Building Technology Journal*, 8, 248-261, 2014.

[12] Iovane G., Noviello C., Mazzolani F.M., Landolfo R., Faggiano B.. Beam-to-column joint with steel link for timber structures: system optimization through numerical investigations and design criteria. *World Conference on Timber Engineering (WCTE2021)*, Santhiago del Chile, Chile, August 9-10, 2021.

[13] EN 1993: 2005: Eurocode 3: Design of steel structures. Part 1-1: General rules and rules for buildings, Part 1-8: Design of joints (CEN: Comité Européen de Normalisation).

[14] Lee C.H. Seismic Design of Rib-Reinforced Steel Moment Connections based on Equivalent Strut Model. *Structural Engineering*, 128 (9), 1121-1129, 2002.

[15] CNR DT 206–R1/2018,. Instructions for the Design, Execution and Control of Timber Structures. Technical document CNR (National Research Council), 2018.

[16] EN 12512: 2001/A1: 2005: Timber Structures - Test methods - Cyclic testing of joints made with mechanical fasteners (CEN, French: Comité Européen de Normalisation).